Electrochemical spectroscopic investigations on the interaction of an ytterbium complex with DNA and their analytical applications such as biosensor

ARTICLE *in* INTERNATIONAL JOURNAL OF BIOLOGICAL MACROMOLECULES · SEPTEMBER 2011

Impact Factor: 2.86 · DOI: 10.1016/j.ijbiomac.2011.09.008 · Source: PubMed

6 AUTHORS, INCLUDING:

Hoda Ilkhani
Utah State University
14 PUBLICATIONS **92** CITATIONS
SEE PROFILE

Majid Arvand
University of Guilan
114 PUBLICATIONS **1,006** CITATIONS
SEE PROFILE

Mohammad Saeid Hejazi
Tabriz University of Medical Sciences
79 PUBLICATIONS **631** CITATIONS
SEE PROFILE

Parviz Norouzi
University of Tehran
494 PUBLICATIONS **8,355** CITATIONS
SEE PROFILE

International Journal of Biological Macromolecules 49 (2011) 1117–1123

Contents lists available at SciVerse ScienceDirect

International Journal of Biological Macromolecules

journal homepage: www.elsevier.com/locate/ijbiomac

Electrochemical spectroscopic investigations on the interaction of an ytterbium complex with DNA and their analytical applications such as biosensor

Hoda Ilkhani[a,b], Mohamad Reza Ganjali[b,c,*], Majid Arvand[a], Mohammad Saeid Hejazi[d,e], Fateme Azimi[b], Parviz Norouzi[b,c]

[a] Department of Chemistry, Faculty of Science, University of Guilan, P.O. Box 1914, Rasht, Iran
[b] Center of Excellence in Electrochemistry, Faculty of Chemistry, University of Tehran, Tehran, Iran
[c] Endocrinology & Metabolism Research Center, Tehran University of Medical Sciences, Tehran, Iran
[d] Faculty of Pharmacy, Tabriz University of Medical Sciences, Tabriz, Iran
[e] Drug Applied Research Center, Tabriz University of Medical Sciences, Tabriz, Iran

ARTICLE INFO

Article history:
Received 6 July 2011
Received in revised form 3 September 2011
Accepted 8 September 2011
Available online 16 September 2011

Keywords:
Differential pulse voltammetry
Cyclic voltammetry
Hybridization
Electrochemical DNA biosensor

ABSTRACT

Metal ion–DNA interactions are important in nature, often changing the genetic material's structure and function. A new Yb complex of $YbCl_3$ (tris(8-hydroxyquinoline-5-sulfonic acid) ytterbium) was synthesized and utilized as an electrochemical indicator for the detection of DNA oligonucleotide based on its interaction with $Yb(QS)_3$. Cyclic voltammetry (CV) and fluorescence spectroscopy were used to investigate the interaction of $Yb(QS)_3$ with ds-DNA. It was revealed that $Yb(QS)_3$ presented an excellent electrochemical activity on glassy carbon electrode (GCE) and could intercalate into the double helix of double-stranded DNA (ds-DNA). The binding mechanism of interaction was elucidated on glassy carbon electrode dipped in DNA solution and DNA modified carbon paste electrode by using differential pulse voltammetry and cyclic voltammetry. The binding ratio between this complex and ds-DNA was calculated to be 1:1. The extent of hybridization was evaluated on the basis of the difference between signals of $Yb(QS)_3$ with probe DNA before and after hybridization with complementary DNA. With this approach, this DNA could be quantified over the range from 1×10^{-8} to 1.1×10^{-7} M. The interaction mode between $Yb(QS)_3$ and DNA was found to be mainly intercalative interaction. These results were confirmed with fluorescence experiments.

1. Introduction

The interaction between DNA and other molecules is an important fundamental issue in life sciences which is related to the replication and transcription of DNA in vivo, mutation of genes and related variations of species in character, action mechanisms of some DNA-targeted drugs, origins of some diseases, and action mechanisms of some synthetic chemical nucleases, etc.

Because of changing the genetic metals structure and function, metal ion–DNA interactions are important in nature. The interaction of DNA with heavy metals has been extensively investigated since they are involved in processes leading to DNA damage [1].

The DNA has four different potential sites for binding of metal ions. These sites are included in the negatively charged phosphate oxygen atoms, the ribose hydroxyls, the base ring nitrogens and the cyclic base keto groups [2]. Most transition metal ions interact with more than two different sites and therefore they have more complicated interactions. They frequently bind indirectly to the phosphate groups and directly to the bases with the N7 atom of purines or N3 of pyrimidines [3].

DNA biosensor for the detection of short sequence DNA makes it possible for people to study organism in molecular level so, it has become an important topic in the fields of gene mutation, disease diagnosis, drug screening and forensic activation analysis [4–9].

Intercalation, first proposed by Lerman et al. [10], is a special binding mode that only happened for ds-DNA. If a small molecule can bind to DNA via intercalation, it often shows stronger binding ability to ds-DNA than to ss-DNA. So, one of the aims for designing the effective discriminator for ss-DNA and ds-DNA is to develop the molecule that can bind to ds-DNA via intercalation. Metallic intercalators are a type of complexes featuring a metal core and an intercalating ligand. Over the past decades, the metallointercalators with polypyridyl ligands have been extensively studied as a kind of nonradioactive nucleic acid probes because of their versatile structures and physicochemical properties [11,12].

* Corresponding author at: Center of Excellence in Electrochemistry, Faculty of Chemistry, University of Tehran, Tehran, Iran. Tel.: +98 21 61112788; fax: +98 21 66405141.
E-mail address: ganjali@khayam.ut.ac.ir (M.R. Ganjali).

0141-8130/$ – see front matter © 2011 Published by Elsevier B.V.
doi:10.1016/j.ijbiomac.2011.09.008

All lanthanides show a marked bioinorganic similarity to Ca^{2+}, with near equivalence of ionic radii, but with a higher charge density. This combination makes displacement of calcium in a physiological milieu a driving concern for many therapeutic and diagnostic applications [13]. They are inner transition elements, defined as the 4f-orbital-filling elements, but also generally including La itself, with electron shell $[Xe]4d^16s^2$. A singular characteristic of the lanthanide series is that the ionic radii contract across the series [14]. As rare earth elements not only have more physiological activity, but also its toxicity is decreased after coordinating with a ligand [15].

Electrochemical methods have also been used to study the interactions of DNA in solution with other molecules, also in solution, which we refer to as solution electrochemical methods [16]. For example, Co(III) [17,18], Fe(II) [18], Ru(II) [19], and Os(II) [20], chelates with 1,10-phenanthroline and 2,2′-bipyridyl bound to DNA have been studied by cyclic voltammetry, differential pulse voltammetry, chronocoulometry, and electrogenerated chemiluminescence. The binding of some antitumor drugs to DNA has been investigated by differential pulse polarography [20]. The limitations of these solution methods include low sensitivity and the need for large samples of DNA, typically milligrams and even more in some cases, which cannot meet the needs of DNA studies, especially gene studies [21–23].

Recently, electrochemical methods, namely modified electrodes, have been used for monitoring the DNA interactions or other molecules [24–27]. Maeda et al. [28] examined the binding of K^+, Na^+, Ca^{2+}, Mg^{2+}, and Ba^{2+} to native DNA on DNA-modified gold electrodes, obtained via self-assembly of DNA having a mercapto group, by indirect electrochemical methods according to their interactions with DNA. They found that DNA-modified electrodes bind these metal ions in the order of Mg^{2+}, Ca^{2+}, Ba^{2+}, K^+, Na^+. Barton and co-workers [29] reported on a gold electrode derivative with 15-base-pair double stranded DNA oligonucleotides containing a pendant 5′-hexanethiol linker.

The hybridization between complementary DNA strands has been usually used as a bio-recognition event for the design of DNA biosensor due to its intrinsic specificity [30,31]. Electrochemical DNA hybridization detection methods are mainly classified into two direct and indirect protocols. Signal transduction induced directly from oxidation of guanine or adenine moieties in DNA strands (label-free detection), while indirect DNA hybridization detection method is based on the incorporation of an electro active label [32,33]. Recently labels have been used for detection of target DNA in PNA/ds-DNA helices and also BCB and haematoxylin have been employed for detection of DNA samples [34–37].

In this work for the first time we study the interaction between $Yb(QS)_3$ and double strand DNA (ds-DNA) with electrochemical and fluorescence methods in biological pH (pH 7). $Yb(QS)_3$ is completely soluble in this pH and we used a ds-DNA for in solution investigations.

To our knowledge, there are no studies exploiting the redox behavior for investigations into the interactions between lanthanides complexes and ds-DNAs with electrochemical methods. The electrochemical methods can study the DNA metal complex interactions and the charges in the electronic properties caused by metal complexes association to DNA that have fundamental importance to biochemistry and analytical biochemistry. The used DNA in this study is a sequence of KMT1 gen. Five capsular types (A, B, D, E, and F) have been recognized in *Pastuerella multocida* based on IHA test and multiplex PCR system [38]. *P. multocida* types A and B are associated with bovine pneumonia and haemorrhagic septicaemia, respectively. Townsend et al. [39] reported KMT1 gene is a species specific region of *P. multocida*. The KMT1 gene of is highly conserved between the capsular serotype A and the capsular serotype D of *P. multocida* [40] and consequently can be used for type and species-specific identification of *P. multocida*.

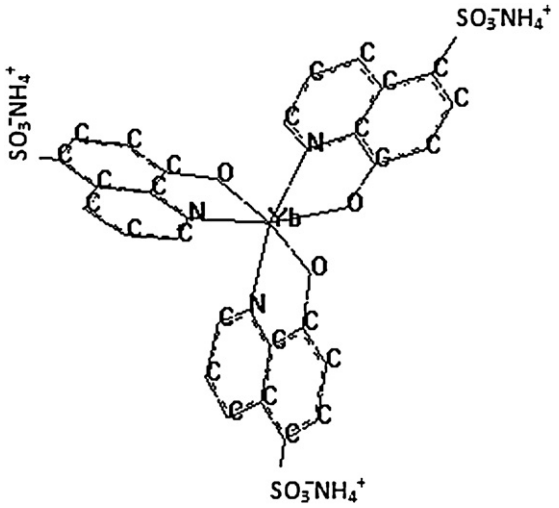

Scheme 1. The molecular structure of $Yb(QS)_3$.

Electrochemical behavior of $Yb(QS)_3$ was studied in pH 7 by cyclic voltammetry method and then the interaction of $Yb(QS)_3$ with a short double strand DNA (ds-DNA) sequence was investigation by cyclic voltammetry and differential pulse voltammetry methods. The constant ratio of complex and binding number of $Yb(QS)_3$ to ds-DNA in this pH was also calculated. The fluorescence studies confirm these results. These evidences indicate that, this complex can be used such as an efficient and sensitive electro active indicator for direct monitoring of DNA hybridization.

2. Experimental

2.1. Material and reagents

$Yb(QS)_3$ (tris(8-hydroxyquinoline-5-sulfonic acid) ytterbium) is a complex of lanthanides and it was synthesized in this way: an ethanol solution of $YbCl_3$ was added to an ethanol solution of HQS (tris(8-hydroxyquinoline-5-sulfonic acid) hydride) while stirring with the molar ratio of Yb^{3+}/HQS being 1:3. Then the pH of solution was adjusted to 7.0 by adding a 2 N ammonium hydroxide solution and an appropriate amount of water was added and the mixture was stirred at room temperature for 10 h. The obtained precipitates were collected by filtration and washed with water and cold ethanol three times (Scheme 1).

Tris–HCl buffer (0.01 M, pH 7 at 25 °C) is received from Sigma. The synthetic oligonucleotides were received (as lyophilized powder) from MWG-Biotech and their base sequences were: immobilized probe 5′-GTG GCG AGT TCG TTT ACA G-3′; target 5′-CTG TAA ACG AAC TCG CCA C-3′; non-complementary 5′-CAT TTA TCC AAG CTC CAC C-3′. The synthetic ds-DNA was prepared in our lab by using of single stranded DNA.

2.2. Preparation of $Yb(QS)_3$ and ds-DNA

Stock solution of $Yb(QS)_3$ was prepared with Tris–HCl buffer (pH 7.0) and DNA stock solutions (1 mM) were prepared with Tris–HCl buffer (pH 7.0) containing 10 mM NaCl and kept frozen at −20 °C temperature until use.

2.3. Instrumentation

Cyclic voltammetry (CV) and differential pulse voltammetry (DPV) were performed using palmsense electroanalyzer system.

All voltametric experiments were carried out at room temperature ($25 \pm 2\,^{\circ}C$) and was used of three electrode system include of 1 ml glassy cell and platinum wire as counter electrode, Ag/AgCl/3 M KCl as the reference electrode. For investigation of interaction between ds-DNA and $Yb(QS)_3$ in solution, the glassy carbon electrode (GCE) was used as the working electrode and for investigation of the same interaction on surface electrode, the carbon paste electrode was used. GC electrode was polished with 0.3 μm (grain size) alumina powder (Metrohm) on a polishing cloth, then it was thoroughly rinsed with water. Carbon paste electrode (CPE) was used for immobilization and hybridization of ss-DNA.

Fluorescence emission and excitation were measured with Perkin Elmer luminescence spectrometer, and the light source was a high pressure xenon lamp. The instrument was free of drift over a 4-h measuring period and relatively noise free at the sensitivities used. Excitation and emission slits was 10 and 10 nm, a respectively gave adequate resolution and good sensitivity.

2.4. Lanthanide-ds-DNA electrochemical investigation

For electrochemical investigation, the $Yb(QS)_3$ solutions were transferred into an electrochemical cell and then the CV and DPV detections/measurements were carried out. All CV experiments were carried out in a potential ranging from −0.6 to 1.2 V, and the scanning rate was $0.1\ V\ s^{-1}$. In DPV studies the interaction between the ds-DNA and $Yb(QS)_3$ was conducted in constant concentration of $Yb(QS)_3$ and various amounts of ds-DNA. All experiments were carried out at the laboratory temperature (25 °C).

2.5. Lanthanide-ds-DNA fluorescence spectroscopy

A 5×10^{-4} M solution of $Yb(QS)_3$ in Tris–HCl buffer (pH 7) was prepared in 3 ml volume. The solution was then titrated with (Tris buffer, pH 7) in different amount of ds-DNA solution to determine the fluorescence enhancement over that of $Yb(QS)_3$ alone in the same condition. The ds-DNA solutions were added to $Yb(QS)_3$ just prior to measurement. This way was especially important with single-stranded DNA samples, since lanthanides slowly catalyze hydrolysis of their inter nucleotides bonds [41].

2.6. Preparation and electrochemical pre-treatment of the carbon paste electrode (CPE)

Carbon paste electrode was prepared in the usual way by hand-mixing of 0.4 g nujol oil and graphite powder in a total of 0.75 g. The resulting paste was packed tightly into a glass sleeve. Electrical contact was established with a copper wire. The surface was polished to a smooth finish before use. The constructed electrode was washed twice with distilled water.

The electrochemical pre-treatment of the surface of polished CPEs was carried out at optimized potential of 1.80 V for 300 s in 0.50 M acetate buffer solution (pH 4.8) containing 20 mM NaCl without stirring. In this experiments *E*-pulse was 0.25, *t*-pulse was 0.05 and *E*-step was 0.0051. This electrochemical instrument parameter was used for all of the following experiments.

2.7. Probe immobilization on the PGE

After electrochemical pretreatment of CPE, the immobilization of the probe was conducted. For this purpose, the electrode was exposed to 0.6 V for 400 s in 0.50 M acetate buffer solution (pH 4.8) containing 1 μM DNA probe and 20 mM NaCl with 200 rpm stirring. The electrode was then rinsed with 0.5 M acetate buffer solution (pH 4.8) containing 20 mM NaCl.

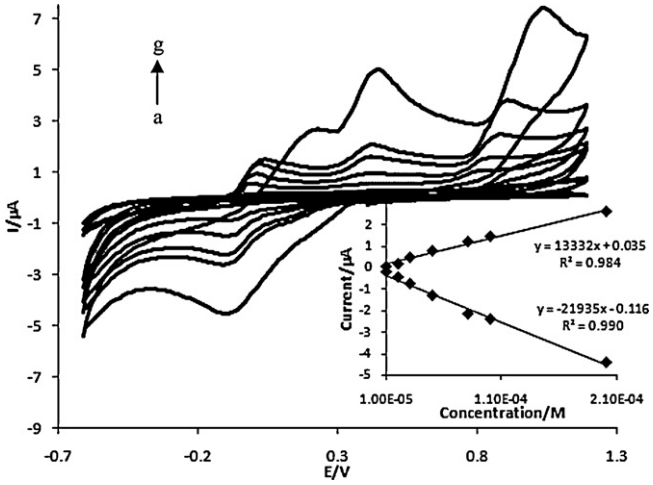

Fig. 1. CVs of: (a) 1.0×10^{-5} M, (b) 2.0×10^{-5} M, (c) 3.0×10^{-5} M, (d) 5.0×10^{-5} M, (e) 8×10^{-5} M, (f) 1.0×10^{-4} M and (g) 2.0×10^{-4} M of $Yb(QS)_3$ in Tris–HCl buffer (pH 7) and scan rate, 100 mVs^{-1}. Inset: plot of I_p *vs.* concentration of $Yb(QS)_3$ in the above condition.

2.8. DNA hybridization

After immobilization of the probe, the electrode was immersed in Tris–HCl buffer solution (pH 7.0) containing 1 μM of target ss-DNA and 20 mM NaCl for ds-DNA helix formation via applying of 0.3 V potential during 500 s. Then, the electrode was washed in 20 mM Tris–HCl buffer solution (pH 7.0) containing 20 mM NaCl (washing solution) for 200 rpm stirring during 300 s. The same procedure was applied for interaction between the probe and non-complementary DNA samples.

3. Result and discussion

3.1. Study of electrochemical behavior of $Yb(QS)_3$

The ytterbium-centered complex has clear electrochemical signals, because of the strong and easy electron donation acceptance properties between Yb(III) and Yb(IV) as redox behavior of ytterbium complexes have not been investigated extensively, the mechanistic aspects of redox behavior of most of them still remain largely uncovered. Generally the redox behavior of the complexes depends on some factors such as: the chelate ring size, axial ligation, degree and distribution of unsaturation and substitution pattern in the chelate ring [42–45]. In the present study, we attempted to use cyclic voltammeteric measurements for understanding redox behavior of $Yb(QS)_3$.

Fig. 1 shows the cyclic voltammograms of $Yb(QS)_3$ complex at different concentrations (from 1×10^{-5} to 2×10^{-4} M) in 0.1 M Tris–HCl buffer solution (pH 7.0) with $0.1\ V\ s^{-1}$ scan rate. The pair quasi-reversible peaks in 0.924 V and 0.816 V can be attributed to Yb (III/IV) oxidation and reduction, respectively. Other peaks are relative to oxidation and reduction of the ligand [29]. The plot of I_p versus concentration of $Yb(QS)_3$ complex is linear (inset in Fig. 1).

Fig. 2 shows the CVs of this complex in different scan rates. The scan rates are ranging between 0.01 and $0.5\ V\ s^{-1}$. As can be seen in this figure by increasing scan rate the redox signal increase markedly and also E_{pc} and E_{pa} are independent of scan rate. In reversible wave, I_p (as well as the current at any other point on the wave) is proportional to $\nu^{1/2}$ (inset in Fig. 2), indicating surface control process.

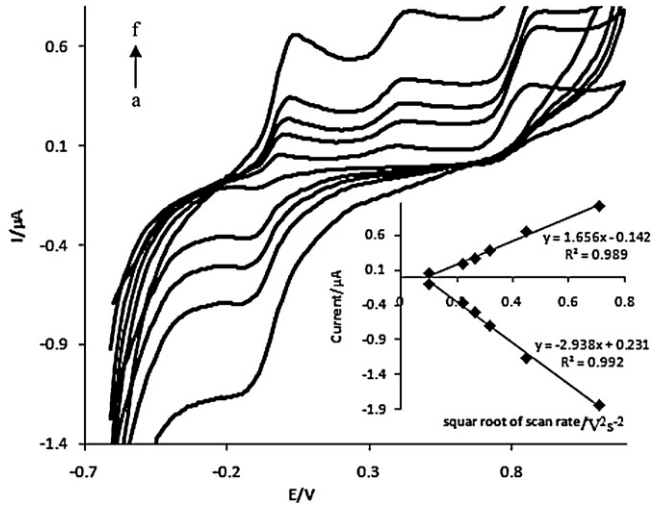

Fig. 2. CVs of: 2.0×10^{-5} M $Yb(QS)_3$ in Tris–HCl buffer (pH 7) with: (a) 0.01 V s^{-1}, (b) 0.05 V s^{-1}, (c) 0.07 V s^{-1}, (d) 0.1 V s^{-1}, (e) 0.2 V s^{-1} and (f) 0.5 V s^{-1} scan rates. Inset: plot of I_p *vs.* square root of scan rates in the above condition.

3.2. Electrochemical investigation of $Yb(QS)_3$ with ds-DNA

To provide evidence about interaction of $Yb(QS)_3$ complex with, the DPV was recorded, comparing the changes of the $Yb(QS)_3$ complex signals before and after the interaction. For preparation of ds-DNA solution, same concentrations of both complementary ss-DNA samples were mixed and boiled until 90 °C, and then the temperature was decreased to room temperature. DPVs of $Yb(QS)_3$ complex in the absence and presence of ds-DNA are shown in Fig. 3. As seen, the peak current decreased with increasing concentration of ds-DNA while formal potential shifted to more positive potentials. The phenomena of the shift of formal potential and the decrease of peak current indicate forming a new association complex between ds-DNA and $Yb(QS)_3$. Among the three kinds of interactions between small molecules and ds-DNA, Carter et al., has reported [46] that if $E^{0'}$ shifts to more negative values following interaction of the small molecules with DNA, the interaction mode are electrostatic binding. On the contrary, if $E^{0'}$ shifts to more positive values the interaction mode is intercalative. As can be seen in Fig. 3, with increasing the ds-DNA concentration, I_p was decreased and the E_p shifted to more positive values (from 0.00 to 0.12 V). Therefore, the conclusion that the $Yb(QS)_3$ complex could intercalate into the base pairs of ds-DNA was obtained.

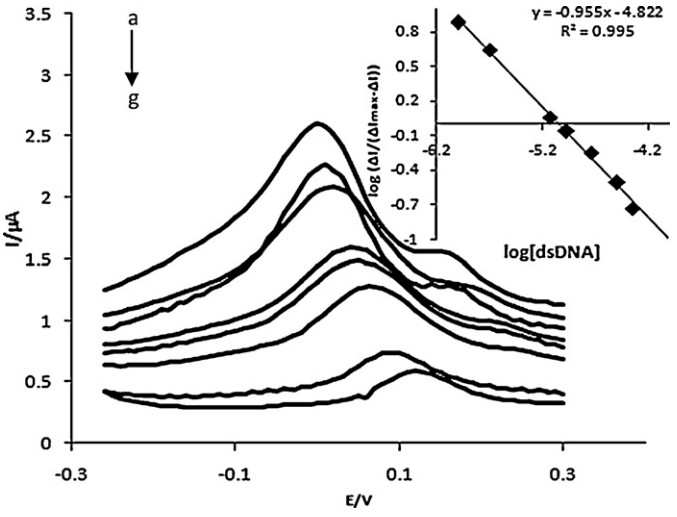

Fig. 3. DPVs of: (a) 5.0×10^{-4} M $Yb(QS)_3$, (b) $a + 2.0 \times 10^{-6}$ M ds-DNA, (c) $a + 7.4 \times 10^{-6}$ M ds-DNA, (d) $a + 1.07 \times 10^{-5}$ M ds-DNA, (e) $a + 1.80 \times 10^{-5}$ M ds-DNA, (f) $a + 3.2 \times 10^{-5}$ M ds-DNA and (g) $a + 4.5 \times 10^{-5}$ M ds-DNA in Tris–HCl buffer (pH 7). The initial potential, −0.25 V, the end potential, 0.3 V, the step potential, 0.015 V, the modulation time, 0.02 s, the interval time, 0.53 s. Inset: plot of $\log[\Delta I/(\Delta I_{max} - \Delta I)]$ *vs.* log[ssDNA] in pH, 7 and the same condition.

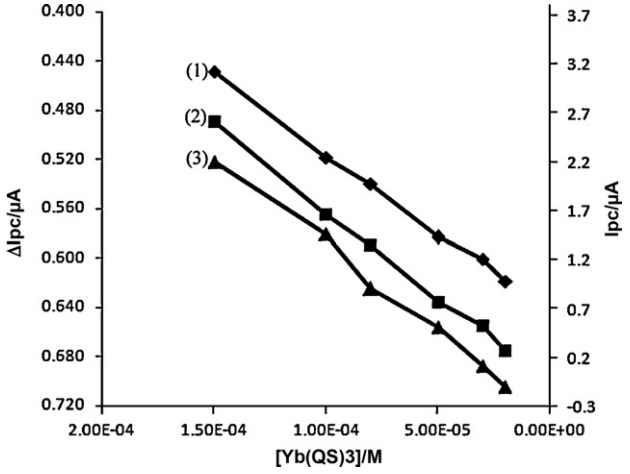

Fig. 4. Curves of reduction peak of $Yb(QS)_3$ (I_{pc}), and ΔI_{pc} *vs.* concentration of $Yb(QS)_3$; (1) concentration of ds-DNA is 0, (2) concentration of ds-DNA is 7.4×10^{-6} and (3) $\Delta I_{pc} = I_{pc}$ (1) − I_{pc} (2).

Fig. 3, with increasing the ds-DNA concentration, I_p was decreased and the E_p shifted to more positive values (from 0.00 to 0.12 V). Therefore, the conclusion that the $Yb(QS)_3$ complex could intercalate into the base pairs of ds-DNA was obtained.

For investigation of binding ratio of the ds-DNA/$Yb(QS)_3$ complex, it was assumed that DNA and $Yb(QS)_3$ only produce one single complex [47] as ds-DNA-n[$Yb(QS)_3$].

If $Yb(QS)_3$ and ds-DNA form a single complex, then the plot of $\log[\Delta I/(\Delta I_{max} - \Delta I)]$ *vs.* log[dsDNA] become linear line with a slope of *n* [47]. Inset in Fig. 3 indicates a linear relationship which implies that $Yb(QS)_3$ can form single complex with ds-DNA in different concentrations of ds-DNA. The slop of this equation is −0.955, the intercept is −4.822 with correlation coefficient *R*, 0.995. The slope value shows that only one $Yb(QS)_3$ complex binds to each ds-DNA. Also value of binding constant, β_s, 1.51×10^{-5} M^{-1} can be obtained in this equation.

Also the following procedure was used for confirmation of the previous results. In this way the following equation was used:

$$\frac{1}{\Delta I_{pa}} = \frac{1}{\Delta I_{pa,max}} + \frac{1}{\beta \Delta I_{pa,max}[Yb(QS)_3]^n} \quad (1)$$

In this equation, ΔI_{pa} is the difference between peak current in the presence and absent of ds-DNA. According to this equation, different *n* can result different curves of $1/\Delta I_{pa}$ *vs.* $1/[Yb(QS)_3]^n$. With the suitable *n*, this curve should be a straight line and therefore could be regarded as the binding ratio. Fig. 4 shows the ΔI_{pa} related to different concentrations of $Yb(QS)_3$ in absent (curve 1) and present (curve 2) of ds-DNA. The relationship between ΔI_{pa} (the difference of I_{pa} in curve 1 and curve 2) and the concentration of $Yb(QS)_3$, was shown in curve 3, when 7.4×10^{-6} M of ds-DNA was added.

Fig. 5 shows the amount of $1/\Delta I_{pa}$ *vs.* $1/[Yb(QS)_3]^n$, in different amounts of *n* (*n* = 0.5, 1, 2). This figure shows that a linear relationship between $1/\Delta I_{pa}$ and $1/[Yb(QS)_3]$, when, *n*, is one (*R* = 0.993). While *n* is one, the curve is a straight line, indicating formation of a 1:1 association between $Yb(QS)_3$ and ds-DNA.

3.3. Fluorescence study of interaction between $Yb(QS)_3$ and ds-DNA

$Yb(QS)_3$ has a fluorescence (emission) spectrum with λ_{max} at 359.5 nm (Fig. 6(a)). To further reveal the possible intercalation binding of $Yb(QS)_3$ with ds-DNA, the fluorescence spectra of $Yb(QS)_3$ in present of ds-DNA was studied. The fluorescence of

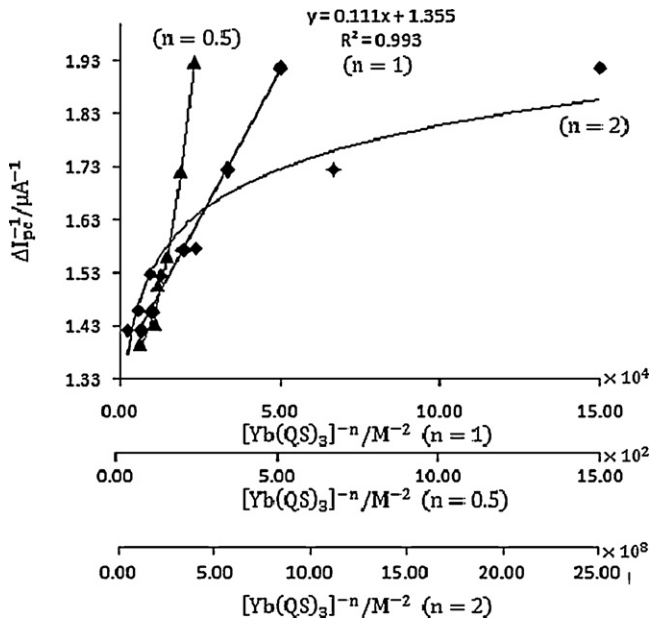

Fig. 5. Curves of $1/\Delta I_{pa}$ *vs.* $[Yb(QS)_3]^{-n}$ and $n = 0.5$, 1and 2.

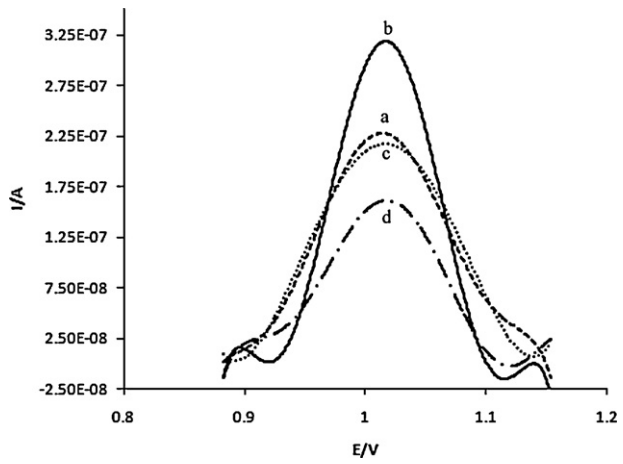

Fig. 7. DPVs of probe-modified PGE before hybridization (a), after hybridization with complementary ss-DNA (b), after hybridization with non-complementary ss-DNA (c), and after accumulation with $Yb(QS)_3$ (d). Experimental conditions were described in Sections 2.7 and 2.8.

ds-DNA was investigated too and there was any peak in this region. Fluorescence titrations of $Yb(QS)_3$ were performed with the use of solutions containing increasing ds-DNA/$Yb(QS)_3$ molar ratios.

To a solution of $Yb(QS)_3$ of a given concentration, ds-DNA was added with increasing concentration, and a fluorescence spectrum of $Yb(QS)_3$ was obtained after each addition of the ds-DNA (Fig. 6). The fluorescence intensity of the main spectral band of the $Yb(QS)_3$ increased with each addition of the ds-DNA and the maximum excitation wavelength of the $Yb(QS)_3$ peak shows a little red shift from 359.5 to 363.5 nm. At relatively high concentration, the peak intensity began to level off. These observations suggest that the binding between ds-DNA and the $Yb(QS)_3$ is relatively strong and the complex, $Yb(QS)_3$–ds-DNA, is formed. Based on the mole ratio method [48], the concentration ratio of $Yb(QS)_3$ and DNA was calculated as 1:1.

3.4. The selectivity of constructed electrochemical DNA biosensor

Because of we could not obtain any peak on GCE surface, Therefore carbon paste electrode (CPE) was used in this section and other next section.

Based upon the above investigated, the $Yb(QS)_3$ complex was further used as an electrochemical indicator for the detection of a synthetic ss-DNA. The selectivity of this assay was explored

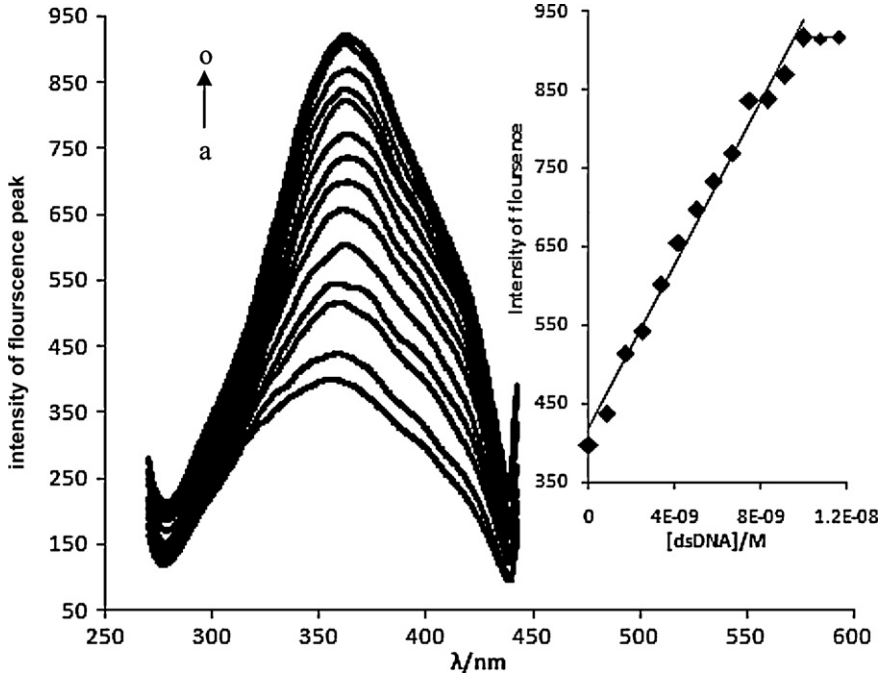

Fig. 6. Enhancement of $Yb(QS)_3$ fluorescence intensity by ds-DNA addition in Tris–HCl buffer (pH 7). A typical excitation (λ_{max} 359.5) spectrum of 1×10^{-8} M $Yb(QS)_3$ complex (a) and different concentration of ds-DNA: (b) $a + 8.30 \times 10^{-10}$ M ds-DNA, (c) $a + 1.68 \times 10^{-9}$ M ds-DNA, (d) $a + 2.5 \times 10^{-9}$ M ds-DNA, (e) $a + 3.32 \times 10^{-9}$ M ds-DNA, (f) $a + 4.17 \times 10^{-9}$ M ds-DNA, (g) $a + 5.0 \times 10^{-9}$ M ds-DNA, (h) $a + 5.8 \times 10^{-9}$ M ds-DNA, (i) $a + 6.65 \times 10^{-9}$ M ds-DNA, (j) $a + 7.5 \times 10^{-9}$ M ds-DNA, (k) $a + 8.3 \times 10^{-9}$ M ds-DNA, (l) $a + 9.15 \times 10^{-9}$ M ds-DNA, (m) $a + 1.0 \times 10^{-8}$ M ds-DNA, (n) $a + 1.08 \times 10^{-8}$ M ds-DNA and (o) $a + 1.17 \times 10^{-8}$ M ds-DNA. Inset: plot of intensity of fluorescence *vs.* concentration of added ds-DNA.

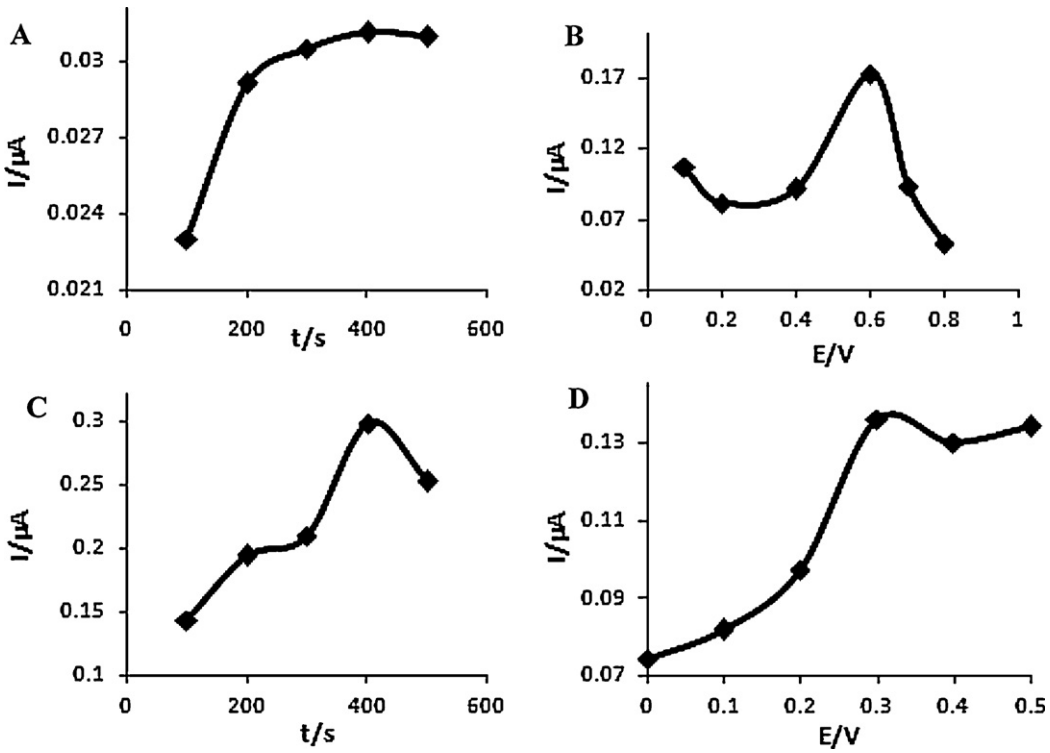

Fig. 8. Variations of current *vs.* (A) probe immobilization times, (B) probe immobilization potential, (C) hybridization time (D) hybridization potential.

by using the ss-DNA/GCE to hybridize with different kinds of DNA sequence. Fig. 7 shows DPV responses of the 1.0×10^{-6} M ss-DNA-modified electrode (curve a), ss-DNA-modified electrode hybridized with non-complementary sequence (curve c) and perfectly matched sequence (curve b). As seen in this figure a significant increase in the voltammetric signals was observed after hybridization of probe ss-DNA modified electrode with the complementary ss-DNA target and After accumulation of $Yb(QS)_3$ on the electrode surface and interaction between ds-DNA and $Yb(QS)_3$ (Fig. 7d), peak slightly decreased so the initial conclusion can be drawn that $Yb(QS)_3$ was interacted with ds-DNA and the interaction mode is intercalative. In addition, this proved that ss-DNA and ds-DNA could be immobilized on the CPE surface, and the target ss-DNA as hybridized with the probe ss-DNA. No significant change in signal was observed when the capture probe ss-DNA was exposed to the non-complementary ss-DNA sequence, in the control experiment, showing the high selectivity of the constructed DNA biosensor for hybridization detection. This further indicated that the $Yb(QS)_3$ could be used as an effective indicator to distinguish between hybrids and non-complementary oligonucleotides for recognizing the target sequence. The interaction of $Yb(QS)_3$ and ds-DNA was mainly the intercalative process.

3.5. Calibration curve

The influence of experimental parameters including the time and potential of immobilization and time and potential of hybridization on the sensitivity of the present method were explored for optimum analytical performance. Fig. 8 shows the optimization condition for these procedures.

The analytical performance of the DNA biosensor was also explored by using the immobilized probe to hybridize with the different concentrations of the complementary sequence according to the described procedure. The peak current increase in DPV responses after hybridization of probe ss-DNA with complementary target ss-DNA could reflect the hybridization extent and be adopted as a measure for DNA hybridization. Fig. 9 shows the calibration plot of DPV responses of $Yb(QS)_3$ for probe DNA modified GCE with different concentrations of complementary target ss-DNA. A linear relationship was obtained up from 1.00×10^{-8} to 1.1×10^{-7} M of complementary target DNA sequences with three independent measurements (Fig. 8). The detection limit of probe ss-DNA modified GCE to its complementary target DNA was achieved to be 6.84×10^{-9} M using 3σ (σ is the standard deviation of blank solution, $n = 4$).

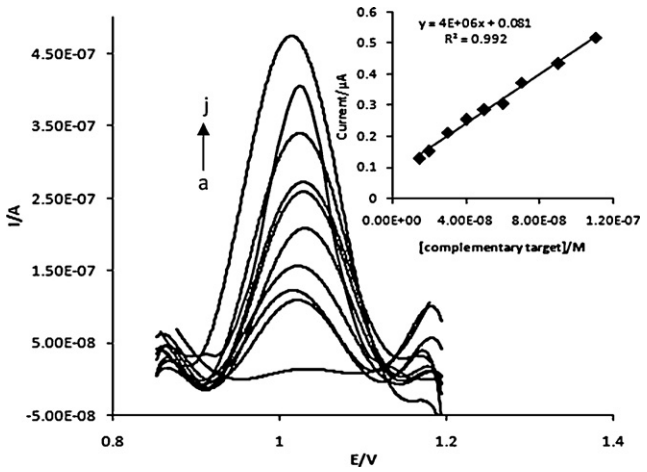

Fig. 9. DPVs of Guanine base of ss-DNA after hybridization with different concentrations of the target sequence. Target concentration ($\times 10^8$ M): (a) 1.5; (b) 2.0; (c) 3.0; (d) 4.0; (e) 5.0; (f) 6.0; (g) 7.0; (h) 9.0; (i) 9.0; (j) 11.0. Insert shows the plot of the peak current as a function of the target concentration. Error bars are ±relative standard deviation.

4. Conclusion

The electrochemical behavior of $Yb(QS)_3$ was investigated in different concentrations and different scan rates. CVs showed a linear correlation between the peak current (I_p) and square root at various scan rates, indicated that the kinetics of process was diffusion-controlled.

The interaction between $Yb(QS)_3$ and ds-DNA was studied using DPV. Results showed that $Yb(QS)_3$ could intercalate into the base pairs of the ds-DNA and binding number obtained one $Yb(QS)_3$ complex per one ds-DNA. The fluorescence evidences supported the electrochemical results. With $Yb(QS)_3$ used as a new electroactive indicator, selectively detection of the short DNA segments was performed. The current respond had a linear relationship with the concentrations of target DNA ranging from 1.00×10^{-8} to 1.1×10^{-7} M and the detection limit was 6.84×10^{-9} M of target DNA. So the utility of a new electrochemical hybridization indicator and developed electrochemical DNA sensor might have promising utilities in clinical application and would lead us to further understanding of the interaction mechanism between antitumor drug and DNA.

References

[1] E. Rojas, L.A. Herrera, L.A. Poirier, P. Ostrosky-Wegman, Mutat. Res. 443 (1999) 157–181.
[2] W. Seanger, Principles of Nucleic Acid Structure, Springer-Verlag, New York, 1984, pp. 201–219.
[3] J. Anastassopoulou, J. Mol. Struct. 651 (2003) 19–26.
[4] D. Leslie, D. Logan, R. Laura, A.M. Elizabeth, D. Sapna, D. Sylvia, Anal. Chem. 79 (2007) 4149–4153.
[5] M.C. Rebeca, S.Á. Patricia, L.C. Jesús, J.M.O. Arturo, T.B. Paulino, Anal. Chem. 79 (2007) 4050–4055.
[6] J. Wang, Nucleic Acids Res. 28 (2000) 3011–3016.
[7] D. Frank, A.H. Margaret, R.C. Andrew, P.J.H. Séamus, Anal. Chem. 79 (2007) 1153–1157.
[8] F.C. Abreu, M.O.F. Goulart, A.M. Oliveira Brett, Biosens. Bioelectron. 17 (2002) 913–919.
[9] M.O.B. Ana, C.D. Victor, Bioelectrochemistry 64 (2004) 143–150.
[10] L.S. Lerman, J. Mol. Biol. 3 (1961) 18–30.
[11] A. Mihailovic, I. Vladescu, M. McCauley, E. Ly, M.C. Williams, E.M. Spain, M.E. Nuñez, Langmuir 22 (2006) 4699–4709.
[12] J. Sun, S. Wu, Y. An, J. Liu, F. Gao, L.N. Ji, Z.W. Mao, Polyhedron 27 (2008) 2845–2850.
[13] K.H. Thompson, C. Orvig, Chem. Soc. Rev. 35 (2006), 499-499.
[14] J.C.G. Bunzli, C. Piguet, Chem. Soc. Rev. 34 (2005) 1048.
[15] X.A. Chen, Q.C. He, T. Guan, Y.E. Cheng, H.F. Chen, B.K. Xiong, Chin. J. Rare Earths 1 (1995) 70–73.
[16] V.K. Gupta, R. Jain, K. Radhapyari, N. Jadon, S. Agarwal, Anal. Biochem. 408 (2011) 179–196.
[17] M.T. Carter, A.J. Bard, J. Am. Chem. Soc. 109 (1987) 7528–7530.
[18] M.T. Carter, M. Rodriguez, A.J. Bard, J. Am. Chem. Soc. 111 (1989) 8901–8911.
[19] M.T. Carter, A.J. Bard, Bioconjug. Chem. 1 (1990) 257–263.
[20] M. Rodriguez, A.J. Bard, J. Anal. Chem. 62 (1990) 2658–2662.
[21] V.K. Gupta, R. Jain, M.M. Antonijevi, H. Khani, M.N. Siddiqui, A. Dwivedi, R. Mishra, S. Agarwal, Int. J. Electrochem. Sci. 6 (2011) 37–51.
[22] S.K. Srivastava, V.K. Gupta, S. Jain, Electroanalysis 8 (1996) 938–940.
[23] A.K. Jain, V.K. Gupta, B.B. Sahoo, L.P. Singh, Anal. Proc. Anal. Commun. 32 (1995) 99–101.
[24] R.N. Goyal, V.K. Gupta, S. Chatterjee, Talanta 76 (2008) 662–668.
[25] A.K. Jain, V.K. Gupta, L.P. Singh, P. Srivastava, J.R. Raisoni, Talanta 65 (2005) 716–721.
[26] R. Prasad, V.K. Gupta, A. Kumar, Anal. Chim. Acta 508 (2004) 61–70.
[27] O. Vrana, V. Brabec, Bioelectrochem. Bioenerg. 19 (1988) 145–160.
[28] M. Maeda, K. Nakano, S. Uchida, M. Takagi, Chem. Lett. 180 (1994) 5–1808.
[29] S.O. Kelley, J.K. Barton, N.M. Jackson, M.G. Hill, Bioconjug. Chem. 8 (1997) 31–37.
[30] R.P. Monica, G. Tania, L. Encarnacion, P. Felix, Biosens. Bioelectron. 22 (2007) 2675–2681.
[31] E. Palecek, M. Fojta, Anal. Chem. 73 (2001) 74A–83A.
[32] C. Ding, F. Zhao, M. Zhang, S. Zhang, Bioelectrochemistry 72 (2008) 28–33.
[33] M.I. Pividori, A. Merkoçi, S. Alegret, Biosens. Bioelectron. 15 (2000) 291–303.
[34] M.S. Hejazi, M.H. Pournaghi-Azar, E. Alipour, E.D. Abdolahinia, S. Arami, H. Navvah, Electroanalysis 3 (2) (2011) 503–511.
[35] M.H. Pournaghi-Azar, F. Ahour, M.S. Hejazi, Anal. Bioanal. Chem. 397 (2010) 3581–3587.
[36] N. Nasirizadeha, H.R. Zare, M.H. Pournaghi-Azar, M.S. Hejazi, Biosens. Bioelectron. 26 (2011) 2638–2644.
[37] M.S. Hejazi, J.B. Raoof, R. Ojani, S.M. Golabi, E. Hamidi-Asl, Bioelectrochemistry 78 (2010) 141–146.
[38] M. Harper, J.D. Boyce, B. Adler, FEMS Microbiol. Lett. 265 (2006) 1–10.
[39] K.M. Townsend, A.J. Frost, C.W. Lee, J.M. Papadimitriou, H.J. Dawkins, J. Clin. Microbiol. 36 (1998) 1096–1100.
[40] D. Sun, J. Wang, R. Wu, C. Wang, X. He, J. Zheng, H. Yang, Vet. Res. Commun. 34 (2010) 649–657.
[41] G.L. Eichorn, J.J. Butzow, Biopolymers 3 (1965) 79–94.
[42] E.K. Barefield, G.M. freeman, D.G. Van Derveer, Inorg. Chem. 25 (1986) 552–558.
[43] P.A. Connick, K.A. Macor, Inorg. Chem. 30 (1991) 4654–4663.
[44] A.M. Tait, F.V. Lovecchio, D.H. Busch, Inorg. Chem. 16 (1977) 2206–2212.
[45] J.A. Streeky, D.G. Pillsbury, D.H. Busch, Inorg. Chem. 19 (1980) 3148–3159.
[46] M.T. Carter, M. Rodriguez, A.J. Bard, Am. Chem. Soc. 111 (1989) 8901–8911.
[47] F. Qu, N.Q. Li, Y.Y. Jiang, Microchem. J. 58 (1998) 39–51.
[48] J.H. Yoe, A.L. Jones, Ind. Eng. Chem. Anal. Ed. 16 (1944) 111–115.